In situ combustion measurements of CO_2 by use of a distributed-feedback diode-laser sensor near 2.0 μm

Michael E. Webber, Suhong Kim, Scott T. Sanders, Douglas S. Baer, Ronald K. Hanson, and Yuji Ikeda

High-resolution absorption measurements of CO_2 were made in a heated static cell and in the combustion region above a flat-flame burner for the development of an *in situ* CO_2 combustion diagnostic based on a distributed-feedback diode laser operating near 2.0 μm. Calculated absorption spectra of high-temperature H_2O and CO_2 were used to find candidate transitions for CO_2 detection, and the $R(50)$ transition at 1.997 μm (the $\nu_1 + 2\nu_2 + \nu_3$ band) was selected on the basis of its line strength and its isolation from interfering high-temperature water absorption. Measurements of spectroscopic parameters such as the line strength, the self-broadening coefficient, and the line position were made for the $R(50)$ transition, and an improved value for the line strength is reported. The combustion-product populations of CO_2 in the combustion region above a flat-flame burner were determined *in situ* to verify the measured spectroscopic parameters and to demonstrate the feasibility of the diode-laser sensor.

OCIS codes: 280.1740, 300.6260.

1. Introduction

Carbon dioxide is a major product of combustion and an important greenhouse gas. As a major product, CO_2 is an indicator of combustion efficiency, and, as a greenhouse gas, CO_2 might be subject to future regulation in the form of carbon taxes. Thus measurements of CO_2's presence may prove to be useful for combustion-control applications or might be required for monitoring carbon emissions. Unfortunately, affordable sensors that can measure absolute CO_2 concentrations nonintrusively in combustion environments are not yet available.

Previous absorption sensors for CO_2 combustion monitoring include diagnostics that use relatively weak overtone bands near 1.55 μm (Refs. 1–3) and initial measurements near 2.0 μm that use external-cavity diode lasers.[4–6] The measurements near 1.55 μm suffered from weak signal strengths and significant interference from high-temperature water absorption. The latter body of research benefitted from CO_2's strong absorption at 2.0 μm but was restricted to slow scanning rates (<25-Hz repetition) caused by the external-cavity diode laser's mechanical operation and could not access all the isolated CO_2 lines in the band.

The objective of the present research is to develop an *in situ* CO_2 diagnostic for combustion applications that is based on recently available distributed-feedback (DFB) diode lasers operating near 2.0 μm. DFB lasers offer the advantages of high bandwidth (to as high as kilohertz repetition rates[7]), ruggedness, compactness, and affordability, and the longer wavelengths that have become available in the past few years offer access to CO_2's strong absorption band near 2.0 μm. For meeting the objective of this research a candidate CO_2 absorption transition was selected [the $R(50)$ line at 1.997 μm], its fundamental spectroscopic parameters were investigated, and measurements of CO_2's presence in a combustion zone by use of the candidate transition were made to demonstrate the feasibility of the sensor and to verify the spectroscopic measurements.

2. Theory

The fundamental theory governing absorption spectroscopy for narrow-linewidth radiation sources is embodied in the Beer–Lambert law [see Eq. (1), be-

M. E. Webber (webber@navier.stanford.edu), S. Kim, S. T. Sanders, D. S. Baer, and R. K. Hanson are with the High Temperature Gasdynamics Laboratory, Department of Mechanical Engineering, Stanford University, Stanford, California 94305-3032. Y. Ikeda is with the Center for Instrumental Analysis, Department of Mechanical Engineering, Kobe University, Kobe 657-8501, Japan.

Received 23 May 2000; revised manuscript received 28 August 2000.

0003-6935/01/060821-08$15.00/0

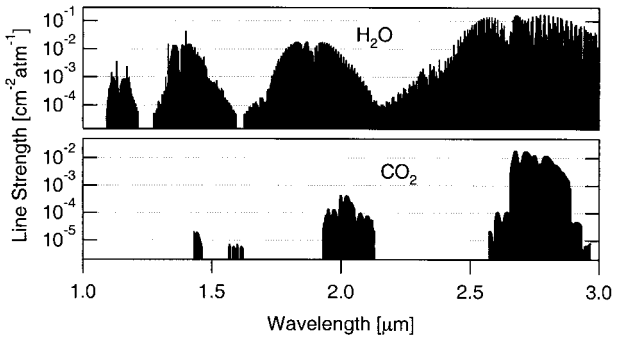

Fig. 1. Calculated water and carbon dioxide line strengths in the near-IR range at 1500 K.[9]

low] and is described thoroughly in Ref. 8. The ratio of the transmitted intensity I_t and the initial (reference) intensity I_0 of laser radiation that passes through an absorbing medium at a particular frequency is exponentially related to the transition line strength S_i (in inverse centimeters squared times inverse atmospheres), the line-shape function ϕ (in centimeters), the total pressure P (in atmospheres), the mole fraction of the absorbing species x_j, and the path length L (in centimeters):

$$\frac{I_t}{I_0} = \exp(-S_i \phi P x_j L). \tag{1}$$

The normalized line-shape function describes the effects of thermal motion (Doppler broadening) and intermolecular collisions (collisional or pressure broadening). The collision width $\Delta\nu_C$ is the FWHM that results from collisions, and at a given temperature is directly proportional to the pressure:

$$\Delta\nu_C = P \sum_B X_B 2\gamma_{A-B}. \tag{2}$$

In Eq. (2), A is the species of interest, P is the total pressure, X_B is the mole fraction of the Bth perturber, and γ_{A-B} is the broadening coefficient for A's transitions by that perturber. For self-broadening the coefficient is often denoted as γ_{A-A} or γ_{self}. The broadening coefficient's temperature variation is often modeled in accord with

$$2\gamma(T) = 2\gamma(T_0)\left(\frac{T_0}{T}\right)^N, \tag{3}$$

where T_0 is a reference temperature, $2\gamma(T_0)$ is the broadening coefficient at the reference temperature, and N is the temperature exponent. The thermal, or Doppler, width $\Delta\nu_D$ is

$$\Delta\nu_D = (7.1623 \times 10^{-7})\nu_{0,i}\sqrt{\frac{T}{M}}, \tag{4}$$

where $\nu_{0,i}$ is the frequency of the transition and M is the mass of the molecule in atomic mass units. For atmospheric pressure the line shape is a convolution of the Doppler and the collisional distributions, yielding a Voigt profile. The Voigt profile is governed by the Voigt a parameter, which relates the thermal and the collisional widths [see Eq. (5)] with a increasing as the line shape becomes more collisionally broadened:

$$a = \frac{(\ln 2)^{1/2}\,\Delta\nu_C}{\Delta\nu_D}. \tag{5}$$

The line strength as a function of temperature for a particular CO_2 transition i is governed by its line strength S_i at a reference temperature T_0, the partition function $Q(T)$ of CO_2, the frequency of the tran-

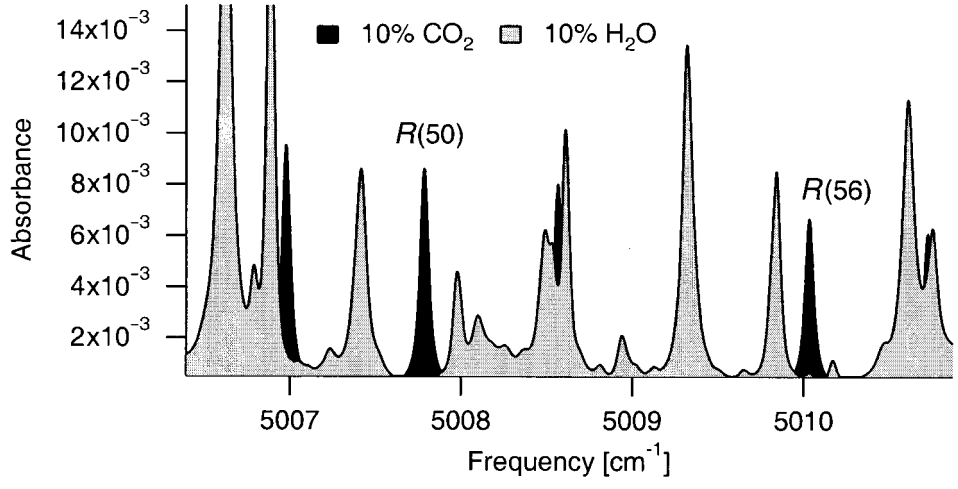

Fig. 2. Calculated spectra of 10% CO_2 and 10% H_2O near 1.997 μm under combustion conditions: $L = 10$ cm, $P = 1$ atm, and $T = 1500$ K. The $R(50)$ and the $R(56)$ transitions of the $\nu_1 + 2\nu_2 + \nu_3$ band at 5007.787 and 5010.035 cm^{-1}, respectively, are partially isolated from high-temperature water interference.

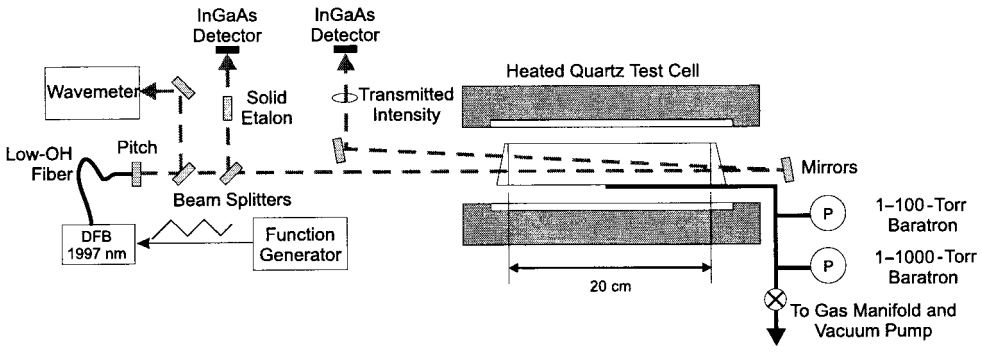

Fig. 3. Schematic diagram of the experimental setup for the measurement of the absorption spectra of CO_2 at a range of pressures and temperatures.

sition $\nu_{0,i}$, and the lower-state energy of the transition E_i''. This relation is given by

$$S_i(T) = S_i(T_0)\frac{Q(T_0)}{Q(T)}\left(\frac{T_0}{T}\right)\exp\left[-\frac{hcE_i''}{k}\left(\frac{1}{T}-\frac{1}{T_0}\right)\right] \times\left[1-\exp\left(\frac{-hc\nu_{0,i}}{kT}\right)\right]\left[1-\exp\left(\frac{-hc\nu_{0,i}}{kT_0}\right)\right]^{-1}. \quad (6)$$

3. Line Selection

Figure 1 graphically depicts the near-IR line strengths of carbon dioxide and water over a range of wavelengths from 1 to 3 μm at a temperature of 1500 K.[9] The absorption bands near 1.55 μm overlap conveniently with commercially available telecommunications diode lasers and thus were used for previous measurements of CO_2. However, as can be seen from Fig. 1, sensors at 2.0 μm can provide access to line strengths that are approximately 2 orders of magnitude larger than those at 1.55 μm. Thus diagnostics that employ these longer wavelengths offer greater sensitivity.

Calculated absorption spectra based on the HITRAN96 database near 2.0 μm were compared for combustion conditions (T = 1500 K, 10% H_2O, 10% CO_2, balance of air, P = 1 atm, and L = 10 cm) and used to find isolated CO_2 transitions. As can be seen from Fig. 2, both the $R(56)$ and the $R(50)$ transitions are relatively isolated and thus are candidate lines for use with a diode-laser absorption sensor. Previous measurements of CO_2 near 2.0 μm employed a research-grade external-cavity diode laser and were restricted to interrogating the $R(56)$ line at 5010.035 cm^{-1} for combustion monitoring.[4,6] However, this transition's absorption records were affected by nonnegligible spectral interference from neighboring high-temperature H_2O lines and required complicated 7-line Voigt fits to extract the partial pressure of CO_2. The $R(50)$ transition offers stronger absorption and superior isolation from high-temperature H_2O spectra in combustion environments than does the $R(56)$ line and thus was selected for the diode-laser sensor in this study.

4. Experimental Setup

Figure 3 shows the basic experimental setup that was used for the static-cell measurements. The diode-laser system consisted of a fiber-pigtailed DFB diode laser operating near 1.997 μm, quartz beam splitters and windows, mirrors, lenses, and extended-

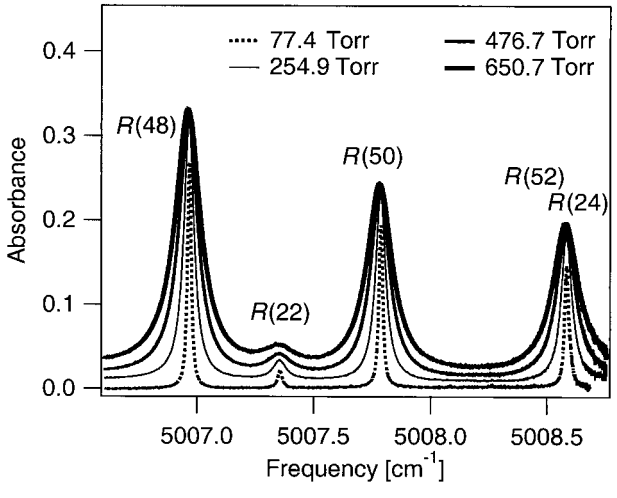

Fig. 4. Absorbance of pure CO_2 for various pressures near 5008 cm^{-1} at T = 294 K and L = 40 cm.

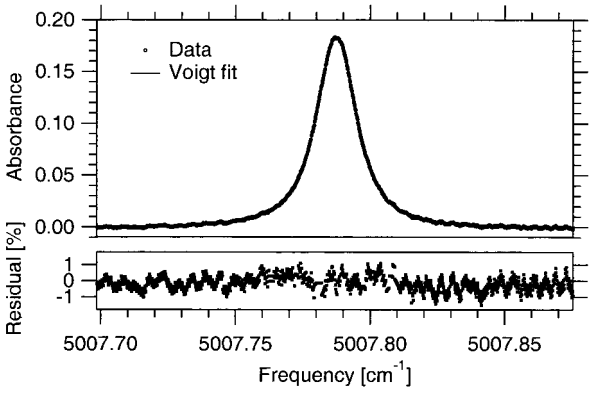

Fig. 5. Sample line shape for static-cell measurements of CO_2 absorbance at 5007.787 cm^{-1} for the $R(50)$ transition with P = 68.1 Torr, L = 40 cm, and T = 294 K.

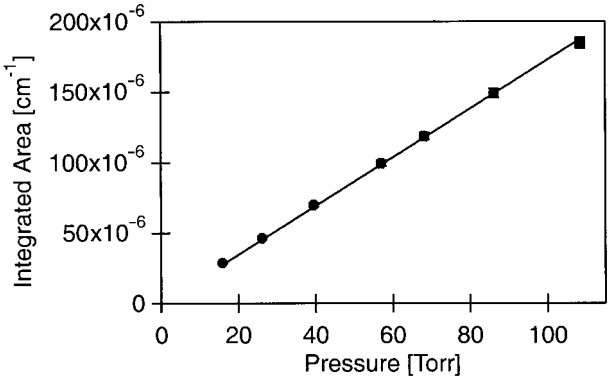

Fig. 6. Measured integrated absorbance area plotted versus the CO_2 pressure at $T = 294$ K for the $R(50)$ line at $\nu_0 = 5007.787$ cm^{-1}. The line strength for this transition is inferred from the slope to be 0.001355 cm^{-2} atm^{-1}.

wavelength-response InGaAs detectors for monitoring the laser intensity. We tuned the DFB laser in wavelength over a transition by holding the diode temperature fixed [near 22 °C for the $R(50)$ line] and ramp-modulating the injection current from 30 to 150 mA at 8.5 Hz. The DFB laser output was coupled to low-OH silica fibers to minimize transmission losses that arise from absorption within the fiber and then was pitched with a collimating lens into free space for the cell measurements.

Beam splitters split the fiber output and directed one path to the IR wavelength meter for measuring the laser frequency, one path through the solid etalon (a free spectral range of 2.01 GHz) for monitoring the wavelength variations during laser tuning, and one path through the static cell to monitor CO_2 absorption. A 12-bit digital oscilloscope was used for data acquisition.

Room-temperature measurements were made with the heater turned off and with two different cells and configurations, including a 20-cm quartz cell with a double-pass alignment and a single-pass 50-cm quartz cell. Unwanted interference fringes that were due to etalon effects in the transmission path were avoided by the mounting of 0.5° wedged windows at a 3° angle on the cells. Two MKS Instruments Model Baratron pressure gauges with 100-Torr and 1000-Torr operational ranges and accuracies of ±1% were used to monitor the test-cell pressure. Temperature variation along the cell was <2%, as measured by the traversing of a type S thermocouple through the furnace.

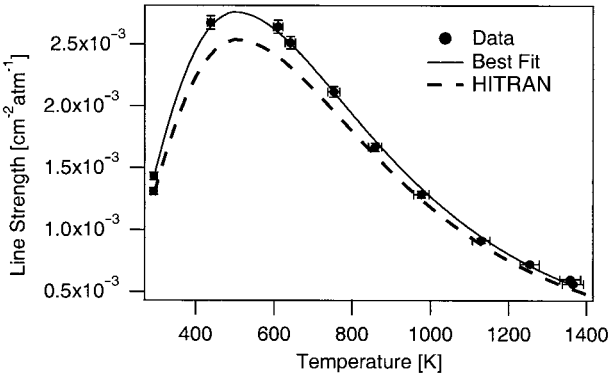

Fig. 7. Line strength plotted versus the temperature for the $R(50)$ transition at 5007.787 cm^{-1}.

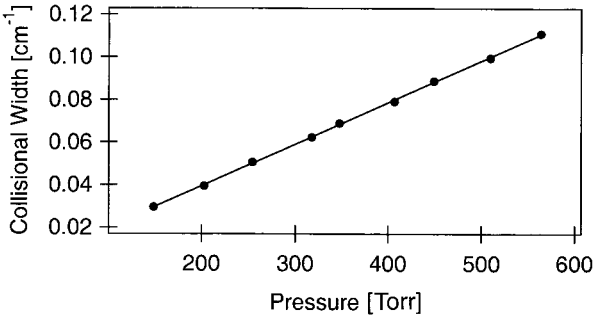

Fig. 8. Measured collisional widths plotted versus the CO_2 pressure at $T = 294$ K for the $R(50)$ line at $\nu_0 = 5007.787$ cm^{-1}. The self-broadening coefficient for this transition is inferred from the slope to be 0.149 cm^{-1} atm^{-1}.

5. Spectroscopic Results

An understanding of the line-strength and the line-shape variations with pressure and temperature aids in the development of CO_2 sensors for combustion environments. Figure 4 shows the results of pressure broadening at room temperature near 5008 cm^{-1} for pure CO_2. At elevated pressures and moderate temperatures neighboring CO_2 transitions can overlap because of strong collisional broadening. Moreover, the line strengths and the broadening (and thus the overlap) will change with temperature. Therefore measurements of the fundamental spectroscopic parameters are important for developing accurate sensors.

Figure 5 shows a typical static-cell absorption line shape overlaid with a best-fit Voigt profile. The peak-normalized residual is less than 2% with a standard deviation of 0.5%, yielding a signal-to-noise ratio of approximately 200, and has no structure, indicating that the Voigt profile adequately models the absorption line shape. The high-frequency component in the residual is likely the result of an accidental etalon in the optical path.

The line strengths at a given temperature were determined by the integration of the area of each Voigt fit to the $R(50)$ transition for a range of pressures between 20 and 150 Torr. The integrated absorbance of an individual transition increases linearly with pressure. Thus the line strength can be determined by the performance of a linear fit on the integrated areas at various pressures, as shown in Fig. 6, and by use of the slope to calculate the line strength. Because zero pressure corresponds to zero absorbance, the linear fit was constrained to pass through the origin.

The total uncertainty for the individual line-strength measurements was estimated to be approximately 3%, resulting from measurement uncertainties

Table 1. Comparison of Measured and Published Parameters for the CO_2 Transitions that Neighbor 5007.787 cm^{-1}

Linecenter[a] ν_0 (cm^{-1})	Transition[b]	Line Strength (cm^{-2} atm^{-1})		Self-Broadening Coefficient (cm^{-1} atm^{-1})		Room-Temperature Line-Strength Uncertainty (%)		Room-Temperature Self-Broadening Coefficient Uncertainty (%)	
		Measured $S_{0,M}$	HITRAN96 $S_{0,H}$	Measured $2\gamma_M$	HITRAN96 $2\gamma_H$	Measured $E_{S,M}$	HITRAN96 $E_{S,H}$	Measured $E_2\gamma_M$	HITRAN96 $E_2\gamma_H$
5006.979	$R(48)$	0.001892	0.001780	0.157	0.1462	3	5	4	20
5007.363	$R(22)$	0.000143	0.000160	0.174	0.1892	3	10	4	10
5007.787	$R(50)$	0.001355	0.001268	0.149	0.1436	3	5	4	20
5008.566	$R(52)$	0.000901	0.000888	0.146	0.1412	3	5	4	20
5008.580	$R(24)$	0.000148	0.000145	0.188	0.1852	3	10	4	10

[a]Values from HITRAN96.
[b]Transition notation: the branch P or R and the lower-state rotational quantum number J''.

of 1% in the total pressure and 2% in the area under each Voigt profile. The room-temperature (294-K) line strength of the $R(50)$ transition was measured to be 0.001355 ± 0.00003 cm^{-2} atm^{-1}, which is approximately 7% higher than the line strength calculated by Rothman *et al.*[10] and listed in HITRAN96 (0.001268 cm^{-2} atm^{-1}). Because the total experimental uncertainty is approximately 3%, compared with 5% for the value in HITRAN96, we consider this measured line strength to be an improvement over the published intensity.

The line strength of the $R(50)$ transition was determined for a range of elevated temperatures, as displayed in Fig. 7. By use of the measured line strengths at various temperatures and Eq. (6) an exponential fit was performed to infer the lower-state energy E'' and to check the accuracy of the transition's quantum assignment (the fit is overlaid in Fig. 7 as a solid curve). The lower-state energy was inferred to be 992 ± 5 cm^{-1}, which agrees with the value from HITRAN96 of 994.1913 cm^{-1} and thereby confirms the line assignment. The measured line strengths are uniformly 7% higher than the values calculated in HITRAN96, which are overlaid as a broken curve in the graph.

The estimated detectivity of the $R(50)$ transition at a combustion temperature of 1500 K and atmospheric pressure is approximately 200 ppm-m (200 parts in 10^6 for a 1-m path length), assuming a noise-equivalent absorbance of 1×10^{-4}. At a typical exhaust temperature of 500 K the detectivity is approximately 50 ppm-m. Other transitions in the 2.0-μm band are more suitable for trace-gas detection at cooler temperatures.

The self-broadening coefficient was measured in a fashion analogous to that of the line strength. Room-temperature absorption measurements were made between 150 and 500 torr, a pressure regime in which the collisional width is larger than the Doppler width, and thus collisional-width estimates are of higher quality. When performing the Voigt fits the Doppler width was held constant at the appropriate value for the measurement temperature. The collisional width was extracted from the overall width of the Voigt fit by use of the calculated Doppler width and the measured Voigt a parameter. The broadening coefficient was determined by the performance of a linear fit on the measured Lorentzian widths at various pressures, as shown in Fig. 8, and by use of the slope to calculate the broadening coefficient [see Eq. (2)]. For the $R(50)$ transition the room-temperature self-broadening coefficient was found to be $2\gamma_{self} = 0.149 \pm 0.004$ cm^{-1} atm^{-1}, which is approximately 4% higher than the value listed in HITRAN96 (0.1436 cm^{-1} atm^{-1}) and 1.5% lower than the published calculation of 0.1514 cm^{-1} atm^{-1},[11] both of which are within our experimental uncertainty.

Self-broadening coefficients for the $R(50)$ transition were determined for temperatures as high as 1400 K, yielding a temperature exponent of $N = 0.521$, which is approximately 1.5% lower than the

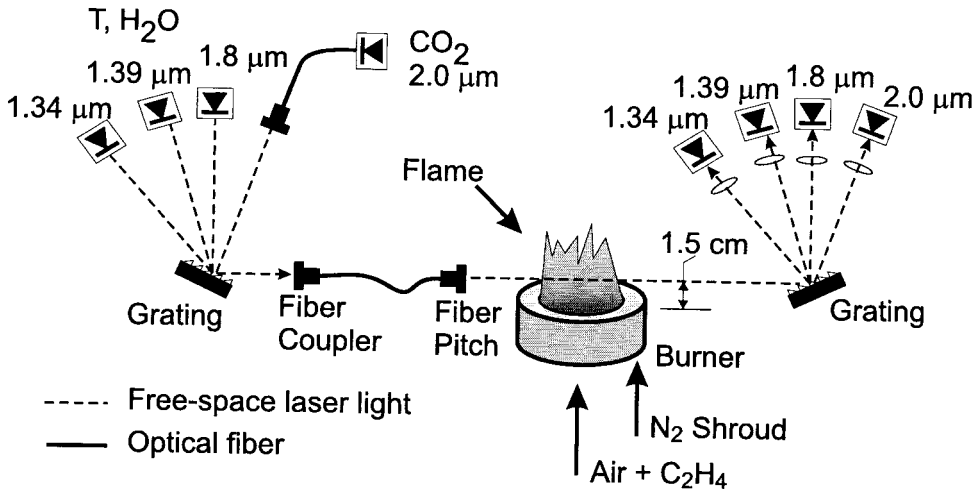

Fig. 9. Schematic diagram of the experimental setup for the *in situ* combustion measurements.

calculated value of 0.529 from Rosenmann *et al.*[11] The total uncertainty for the individual broadening-coefficient measurements was estimated to be approximately 4% as a result of measurement uncertainties of 1% in the total pressure and 3% in the Lorentzian width extracted from each broadened Voigt profile.

Measurements of room-temperature line-strength and self-broadening coefficients were also performed for the neighboring CO_2 transitions between 5007 and 5008.6 cm^{-1}. These spectroscopic parameters are summarized in Table 1 along with published values for comparison. Because these results were obtained with only a 3% experimental uncertainty for the line strength and a 4% uncertainty for the broadening coefficients, it is expected that they are an improvement over the values listed in HITRAN96, which have uncertainties of 5%–10% for the line strengths and 10%–20% for the broadening coefficients. Because the discrepancy between the measured and the published values is not uniform for the different transitions that were investigated in this study, we do not draw any conclusions about the overtone band strength in general. Note that the measured line positions for each of these transitions agreed with the HITRAN96 values within the precision of the IR wavelength meter (0.01 cm^{-1}).

6. Combustion Measurements

Figure 9 shows the experimental setup for the measurements of CO_2 concentration in the combustion region above a flat-flame burner. The 6-cm-diameter flat-flame burner operated on premixed ethylene and air and used a shroud flow of N_2 to flatten the horizontal flame sheet, stabilize the flame's outer edges, and minimize the entrainment of ambient air into the combustion region near the burner's surface.

The flows of ethylene and air were metered with calibrated rotameters. Fixing the air-flow rate (30.9 l/min) and varying the ethylene-flow rate (1.35–3.1 l/min) produced a range of equivalence ratios of $\phi = 0.6–1.44$ (limited by the burner, not the sensor). Uncertainty in the fuel-flow rate, and thus the equivalence ratio, was approximately 2%. The temperature was uniform to within an 8% variation across the plateau, as measured by the tra-

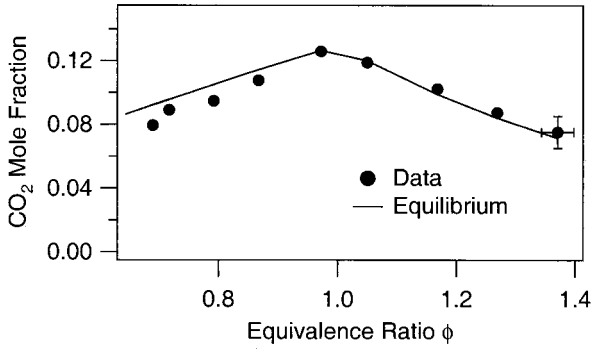

Fig. 10. Comparison of the measured CO_2 mole fraction in the combustion region with equilibrium values. The experimental uncertainty is shown at only one point for clarity.

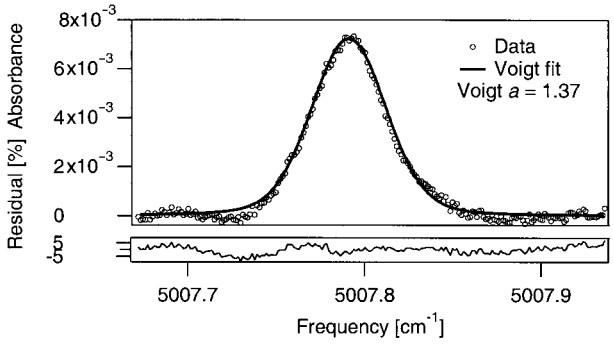

Fig. 11. Sample CO_2 line shape for absorption measurements in the combustion region by use of the $R(50)$ transition with $\phi = 0.79$, $X_{CO_2} = 0.105$, $T = 1690$ K, $P = 1$ atm, and $L = 17$ cm.

versing of a type S thermocouple across the combustion region.

The diode-laser system consisted of multiplexed lasers operating at 1.343, 1.392, 1.799, and 1.997 μm. The output beams from all four lasers were combined into one multimode optical fiber (50-μm core diameter, multimode, low-OH silica) and directed through the combustion region by use of a collimating lens for simultaneous measurements of H_2O, CO_2, and gas temperature along a single optical path (22.8-cm nominal path length, four passes) that was 1.5 cm above the burner surface. The beam was demultiplexed after the combustion region with a diffraction grating (830 grooves/mm, 1.25-μm blaze angle) so that the transmitted intensity from each laser could be monitored independently. Standard and extended-wavelength InGaAs detectors (2-mm detector diameter, 300-kHz bandwidth) were used to record the transmitted-beam intensities.

The lasers were wavelength scanned at 1250 Hz (800 μs/single sweep, 800 points/scan) to minimize beam-steering effects and low-frequency ($1/f$) noise. Detector voltages were sampled at 1 MHz with a 12-bit digital oscilloscope. Signals that were due to flame emission were typically less than 3% of the laser intensity and were subtracted from the transmission signals before analysis of the absorption spectra. The spectroscopic details of the water and the temperature diagnostics are discussed in Sanders *et al.*[12]

The recorded CO_2 mole fractions in the combustion region are displayed in Fig. 10 and overlaid with the equilibrium values at the measured temperatures for equivalence ratios between 0.7 and 1.4. In the lean regime the measured concentrations agree to within 10% of the equilibrium values and in the rich regime to within 5%. Temperature fluctuations and edge effects in the flame (especially in lean conditions), uncertainty in the temperature measurement (3%), and uncertainty in the line strengths (3%) are the largest sources of experimental uncertainty for the concentration measurements, producing an overall uncertainty of approximately 10%.

Figure 11 shows a sample data trace of a recorded CO_2 absorption line shape along with the best Voigt fit and the peak-normalized residual. As the baselines, which corresponded to zero absorbance, were easily determined for this probed CO_2 transition because of its isolation from H_2O interference, single-line Voigt fits were used to determine the integrated area. This isolation and simplicity is an improvement over previous *in situ* measurements of CO_2 that used the $R(56)$ transition near 1.996 μm. Note that the transition used in this study was isolated from CO_2 interference that is due to self-broadening from neighboring low-temperature lines but does show low interference near 5007.7 cm^{-1} from a high-temperature CO_2 line.

7. Conclusions

A CO_2 sensor for combustion environments that used diode-laser absorption techniques has been developed and demonstrated. Calculated high-temperature absorption spectra of CO_2 and H_2O were overlaid to find suitable transitions for *in situ* monitoring, yielding two candidates: the $R(50)$ transition at 5007.787 cm^{-1} and the $R(56)$ transition at 5010.035 cm^{-1}.

The $R(50)$ transition was selected for the CO_2 diagnostic on the basis of its line strength and its isolation from water interference at combustion temperatures. Pertinent spectroscopic parameters (S, ν_0, E'', $2\gamma_{self}$) for this transition were measured and compared with the literature values, resulting in an improved value for a room-temperature line strength with an uncertainty of 3% and a self-broadening coefficient with an uncertainty of 4%. Measurements of CO_2 concentration in the combustion region above a flat-flame burner at atmospheric pressure were made to verify the fundamental spectroscopic parameters and to demonstrate the capacity for *in situ* monitoring by use of diode-laser sensors near 2.0 μm.

This research was primarily supported by the U.S. Environmental Protection Agency's Office of Research and Development's National Center for Environmental Research Science to Achieve Results (STAR) research grants program, with additional support from Metrolaser, Inc., through the Department of Energy Small Business Innovative Research program.

References

1. D. M. Sonnenfroh and M. G. Allen, "Observation of CO and CO_2 absorption near 1.57 μm with an external-cavity diode laser," Appl. Opt. **36,** 3298–3300 (1997).
2. R. M. Mihalcea, D. S. Baer, and R. K. Hanson, "Diode-laser sensor for measurements of CO, CO_2, and CH_4 in combustion flows," Appl. Opt. **36,** 8745–8752 (1997).
3. R. M. Mihalcea, D. S. Baer, and R. K. Hanson, "Diode-laser absorption sensor for combustion emission measurements," Meas. Sci. Technol. **9,** 327–338 (1998).
4. R. M. Mihalcea, D. S. Baer, and R. K. Hanson, "Advanced diode laser absorption sensor for *in-situ* combustion measurements of CO_2, H_2O, and gas temperature," Proc. Combust. Inst. **27,** 95–101 (1998).
5. R. M. Mihalcea, M. E. Webber, D. S. Baer, R. K. Hanson, G. S. Feller, and W. B. Chapman, "Diode-laser absorption measurements of CO_2, H_2O, N_2O, and NH_3 near 2.0 μm," Appl. Phys. B **67,** 283–288 (1998).
6. R. M. Mihalcea, D. S. Baer, and R. K. Hanson, "Diode-laser measurements of CO_2 near 2.0 μm at elevated temperatures," Appl. Opt. **37,** 8341–8347 (1998).
7. E. R. Furlong, D. S. Baer, and R. K. Hanson, "Real-time adaptive control using diode-laser absorption sensors," Proc. Combust. Inst. **27,** 103–111 (1998).
8. V. Nagali, S. I. Chou, D. S. Baer, R. K. Hanson, and J. Segall, "Tunable diode-laser absorption measurements of methane at elevated temperatures," Appl. Opt. **35,** 4026–4032 (1996).
9. L. S. Rothman, C. P. Rinsland, A. Goldman, S. T. Massie, D. P. Edwards, J. M. Flaud, A. Perrin, C. Camy-Peyret, V. Dana, J.-Y. Mandin, J. Schroeder, A. McCann, R. R. Gamache, R. B. Wattson, K. Yoshino, K. V. Chance, K. W. Jucks, L. R. Brown, V. Nemtchinov, and P. Varanasi, "The HITRAN molecular

spectroscopic database and HAWKS (HITRAN atmospheric workstation): 1996 edition," J. Quant. Spectrosc. Radiat. Transfer **60,** 665–710 (1998).
10. L. S. Rothman, R. L. Hawkins, R. B. Wattson, and R. R. Gamache, "Energy levels, intensities, and linewidths of atmospheric carbon dioxide bands," J. Quant. Spectrosc. Radiat. Transfer **48,** 537–566 (1992).
11. L. Rosenmann, J. M. Hartmann, M. Y. Perrin, and J. Taine, "Accurate calculated tabulations of IR and Raman CO_2 line broadening by CO_2, H_2O, N_2, and O_2 in the 300–2400 K temperature range," Appl. Opt. **27,** 3902–3907 (1988).
12. S. T. Sanders, D. S. Baer, and R. K. Hanson, "Diode laser absorption sensor for measurements in pulse detonation engines," in *Proceedings of the Thirty-Eighth AIAA Aerospace Sciences Conference* (American Institute of Aeronautics and Astronautics, New York, 2000), paper 2000-0358.